Glycoconj J (2013) 30:183–194
DOI 10.1007/s10719-012-9396-z

Priming mass spectrometry-based sulfoglycomic mapping for identification of terminal sulfated lacdiNAc glycotope

Shin-Yi Yu · Lan-Yi Chang · Chu-Wen Cheng · Chi-Chi Chou · Michiko N. Fukuda · Kay-Hooi Khoo

Received: 5 March 2012 / Revised: 10 May 2012 / Accepted: 11 May 2012 / Published online: 1 June 2012

Abstract In an effort to prime our mass spectrometry (MS)-based sulfoglycomic mapping platform technology for facile identification of sulfated lacdiNAc (GalNAcβ1-4GlcNAcβ1-), we have re-examined the N-glycans of bovine thyroid stimulating hormone. We showed that MALDI-MS mapping of permethylated glycans in negative ion mode can give an accurate representation of the sulfated glycans and, through MS/MS, diagnostic ions can be derived that we can collectively define the presence of a terminal sulfated lacdiNAc moiety at high sensitivity. Based on these ions, which can also be produced by nanoESI-MS^n, we demonstrated that the glycome of an ovarian carcinoma cell line, RMG-1, comprises a high abundance of sulfated lacdiNAc epitopes carried on multiantennary complex type N-glycans alongside fucosylated, sialylated and/or sulfated lacNAc antennae. This represents the first report of a natural glycomic occurrence of sulfated lacdiNAc on a cell line, as opposed to other better-characterized presence on secreted glycoproteins from a handful of sources. It is anticipated that with improved methods of detection such as that developed in this work, we are likely to identify a wider occurrence of sulfated lacdiNAc and be able to more accurately delineate the regulatory mechanism dictating the choice of a cell type in synthesizing sulfated, sialylated, fucosylated and/or non-substituted lacdiNAc.

Keywords Glycomics · Sulfoglycomics · Mass spectrometry · Glycan sequencing · Sulfated lacdiNAc · bTSH · Ovarian cancer cells

Abbreviations

bTSH	bovine thyroid stimulating hormone
lacdiNAc	*N,N′*-diacetylgalactosediamine (GalNAcβ1-4GlcNAcβ1-)
lacNAc	*N*-acetyllactosamine (Galβ1-4GlcNAcβ1-)
HexNAc	*N*-acetylhexosamine
Hex	hexose
MS	mass spectrometry
CID	collision induced dissociation
HCD	higher energy collision dissociation

S.-Y. Yu · L.-Y. Chang · K.-H. Khoo (✉)
Institute of Biological Chemistry, Academia Sinica,
128, Academia Road Sec 2, Nankang,
Taipei 115, Taiwan
e-mail: kkhoo@gate.sinica.edu.tw

C.-W. Cheng · K.-H. Khoo
Institute of Biochemical Sciences, National Taiwan University,
Taipei 106, Taiwan

C.-C. Chou
Core Facilities for Protein Structural Analysis, NCFPB,
Academia Sinica,
Taipei 115, Taiwan

M. N. Fukuda
Tumor Microenvironmental Program, Cancer Center,
Sanford-Burnham Medical Research Institute,
La Jolla, CA 920137, USA

Introduction

The advent and rapid technical advances of mass spectrometry (MS)-based glycomics made over the last decade or so have precipitated the concept of protein glycosylation analysis on a global scale, aiming to define the glycome of a biological sample in its entirety [1, 2]. Although occasional multifaceted mapping has been attempted to increase the depth and breath of glycomic coverage, most undertakings to date are largely confined to single dimensional profiling,

supplemented by select MS/MS analyses. At times, such analyses yielded impressive correlations between defects in glycosylation machinery and its manifested glycomic phenotype, revealed obvious changes registered upon immune activation and malignant transformation, and allowed attempts in identifying glyco-based biomarkers for diseases and cancer by comparative analyses [3–6]. It is, however, widely appreciated that we often only detect the most obvious changes occurring on those more abundant glycan components. The sulfated N- and O-glycans, for example, are not only less abundant except perhaps in the cases of epithelial and secreted mucins, but also particularly problematic to be detected due to their negative charges.

Recognizing a pressing need in unraveling the distribution of various distinct sulfated glycotopes among myriad glycan carriers, we have taken the lead in developing enabling techniques and strategic workflows for sulfoglycomics [7, 8] based on the well-proven advantages afforded by MS mapping and sequencing of permethylated glycans [9–11]. We demonstrated that the sulfates are largely retained while near complete permethylation can be achieved. The particular strength of this derivatization is that it neutralizes the charge contributed by the sialic acids, thus leaving the sulfated glycans as the only negatively charged glycans left. This allows selective detection in negative ion mode whilst subsequent microscale fractionation can be efficiently carried out to enrich specifically for mono- and higher sulfated glycans from the otherwise overwhelming non-sulfated but sialylated or neutral glycans. Initial efforts were directed towards recovering these sulfated permethylated glycans and to further analyze them in positive ion mode, so as to take advantage of the well defined MS/MS fragmentation pathways for structural determination [10].

Although we have successfully demonstrated the feasibility of this approach against sulfated glycans derived from standard glycoproteins and cell lysates [8], we have since found that the sensitivity is often insufficient in positive ion mode for productive MS/MS, relative to that achieved in negative ion mode for initial MS screening. It was anticipated that MS/MS in negative ion mode would only produce few fragment ions retaining the sulfate and hence not be as comprehensive in giving a full range of fragment ions as in positive ion mode for complete sequencing and definition of core types, branching pattern, and the linkages of terminal glycotopes. However, the few diagnostic ions may be sufficient to allow specific identification of terminal sulfated epitopes. These have in fact been shown by us to be the case for the 6-sulfo sialyl Lewis X epitope carried on the complex type N-glycans [12] and the smaller O-glycans [13]. We are interested to extend this initial observation to include other biologically active sulfated glycotopes, which may have a wider occurrence than currently appreciated. In the absence of corresponding antibodies with well-defined specificities, MS-based sulfoglycomic screening of such epitopes remains the only viable alternative.

Sulfated lacdiNAc, SO_4-4GalNAcβ1-4GlcNAcβ1-, is one of the better known sulfated glycotopes first identified on several pituitary glycohormones, with a well defined role in mediating their clearance from blood circulation via a specific hepatic endothelial GalNAc-4-SO_4 receptor [14, 15]. However, neither the expression of the terminal lacdiNAc itself nor the GalNAc-4-sulfotransferases, which recognize and add a sulfate to the 4-position of the terminal GalNAc, is restricted to pituitary glands. In fact, various non-substituted, sialylated and/or fucosylated lacdiNAc terminal units have been reported to be carried on a wide range of glycoproteins and tissues [16–22]. In contrast, sulfated lacdiNAc has thus far been additionally found on only a handful of glycoproteins from cerebellum [23], submaxillary gland [24], two urinary glycoproteins [25, 26], and recombinant glycoproteins produced in HEK 293 cells [27]. None was reported via a current MS-based glycomic mapping of tissue or cell lysates. It is unclear if it indeed has a more restricted occurrence despite the wider expression range of the identified GalNAc-4-sulfotransferases [28], or likely to have been overlooked due to lack of specific antibody and other enabling detection techniques.

In this report, using the readily available bovine thyroid stimulating hormone (bTSH) as standard bearer of sulfated lacdiNAc [14, 29], we first showed that the kind of cleavage ions usually afforded only by high energy CID TOF/TOF MS/MS in positive ion mode [10] can be similarly produced in negative ion mode analysis of sulfated lacdiNAc-carrying N-glycans and a very characteristic set of ions would allow its unambiguous identification. Intriguingly, through our sulfoglycomic analysis and relying on these diagnostic fragment ions, this particular sulfated glycotope was found to be abundantly expressed on an ovarian cancer cell line, RMG-1, which makes it an attractive model to investigate the functional aspects of this epitope outside the glycohormone targeting context.

Materials and methods

Sample materials and chemicals The standard glycoprotein, bovine thyroid stimulating hormone (bTSH) was purchased from Sigma-Aldrich (Product No. T8931). Ovarian clear cell carcinoma, RMG-I cells, were cultured in Dulbecco's Modified Eagle (DME) high glucose medium/Ham's F12 medium (Life Technologies, Inc., Grand Island, NY) supplemented with 10 % fetal calf serum, as described [30]. N-glycosidase F was purchased from Roche. Other reagents for processing the released N-glycans for MS analysis include dithiothreitol (Sigma-Aldrich), iodoacetamide (Sigma-

Aldrich), trypsin (Bovine Pancreas, TPCK-treated, Sigma-Aldrich, T-1426), C8 Sep-Pak cartridge (Waters, Part No. WAT036775), C18 Sep-Pak cartridge (Waters, Part No. WAT051910), acetonitrile (Merck), methanol (Merck), 1-propanol (Merck), sodium hydroxide (NaOH, Merck, pellets for analysis, ISO grade), dimethyl sulfoxide (DMSO, Merck, purity ≥99.9 %, max 0.025 % H_2O), and methyl iodide (Merck, purity ≥99 %, stabilized with silver for synthesis).

Preparation of N-linked glycans for MS analysis RMG-1 cell pellets were washed with PBS, re-suspended in 100 mM ammonium bicarbonate, boiled for 5 min and then lyophilized. Total N-glycans were released from this material for initial screening following the usual extraction and protease digestion steps as described previously [8]. To enrich further the negatively charged N-glycans, the harvested RMG-1 cells were digested with trypsin and glycopeptides were isolated by passing through Sephadex G-15 in water followed by QAE-Sephadex chromatography, and the collected fractions containing the negatively charged glycopeptides were further desalted by Sephadex G-15 equilibrated with water as described [31]. Permethylation of the N-glycans released from both bTSH and RMG-1 glycopeptides, and the ensuing microscale desalting and fractionation steps were performed without modification according to the standard protocols described previously in detail elsewhere [7, 8]. An aliquot of the RMG-1N-glycans was treated with sialidase (*Arthrobacter ureafaciens*, Calbiochem) in 50 mM ammonium acetate buffer (pH 5.5) at 37˚C overnight, before subjecting to chemical derivatization.

MALDI-MS and MS/MS analysis MALDI-TOF/TOF MS and MS/MS analysis of permethylated glycans were performed on a 4700 Proteomics Analyzer (Applied Biosystems, Framingham, MA) equipped with Nd:YAG laser, operated in the reflectron mode. For MS and MS/MS acquisition, the permethylated samples in acetonitrile were premixed 1:1 with 2,5-dihydroxybenzoic acid (DHB) matrix (10 mg/mL in 50 % acetonitrile) in the positive ion mode, or 1:1 with 3,4-diaminobenzophenone (DABP) matrix (10 mg/mL in 75 % acetonitrile/0.1 % trifluoroacetic acid) (Acros Organics, NJ, USA) in the negative ion mode for spotting onto the target plate. Data acquisition normally comprised 40 sub-spectra of 50 laser shots, and the laser energy was set at 4500. The collision energy for CID MS/MS analysis in positive and negative ion modes was set at 3 kV and 1 kV, respectively.

Offline nano-ESI-MS and MS/MS analysis The permethylated glycans were additionally cleaned up by $ZipTip_{C18}$, eluted in 50 % acetonitrile containing 0.1 % trifluoroacetic acid, and directly loaded into the borosilicate metal (Au) coated glass capillary. nanoESI-MS and MS/MS analysis were performed on an LTQ-Orbitrap Velos hybrid mass spectrometer (Thermo Scientific), with the capillary voltage set at 0.5 kV. The full MS scan was acquired within *m/z* 800–2000 mass range and detected in the Orbitrap mass analyzer at a resolution of 30,000. The MS^n analysis was performed either in the CID mode with normalized collision energy of 35 % and detected in the ion trap, or in HCD mode where the normalized collision energy is set at 90 % and detected in the Orbitrap analyzer at 15000 resolution.

Results and discussion

Overall features exemplified by MALDI-MS mapping of sulfated N-glycans from bTSH

As reported previously [7, 8], our MS-based sulfoglycomic approach relies on efficient permethylation of the released glycans followed by C18 Sep-Pak clean-up and then subject the pooled fractions to negative ion mode MALDI-MS screening. Our experience showed that any sulfated glycan present at a significant level would be revealed and the signal intensity registered is often a guide to subsequent steps of microscale fractionations needed. MALDI-MS mapping of the permethylated glycans in positive ion mode, on the other hand, normally allows detection of only the more abundant neutral and sialylated but not the sulfated glycans, unless the former are largely absent. Such is the case for the sulfated glycan standards, as shown here by both positive and negative ion mode analyses of the released, permethylated total N-glycans from bTSH (Fig. 1).

The N-glycans from bTSH were first characterized in detail by a combination of conventional biochemical approaches without the support of MS analysis [29, 32]. It was concluded then the major structures were hybrid and complex type biantennary N-glycans, with and without core fucosylation, and each antenna terminated with a sulfated lacdiNAc sequence instead of the more common sialylated lacNAc (see annotated structures on Fig. 1). The disulfated biantennary structure with both antennae bearing the sulfated lacdiNAc was deduced to constitute almost half of all released N-glycans, whereas the monosulfated complex type and hybrid type with 0–2 extra mannoses retained on the trimannosyl core represented 12 % and 20 % of the total, respectively. Remarkably, non-sulfated sialylated structures were not detected, in contrast to other pituitary glycohormones. It thus uniquely serves as a gold standard for developing MS analysis methods for sulfated glycans without the added complication of negatively charged sialic acids.

Although the signal intensity afforded by MALDI-MS analysis is not a very accurate index for quantification particularly in the case of comparing species with different

degrees of negative charges, it does give a rough indication of relative abundance. As noted before [8], MALDI-MS analysis of the sulfated N-glycans afforded mostly deprotonated $[M-H]^-$ or monosodiated $[M + Na-2H]^-$ molecular ions in negative ion mode for mono- and disulfated glycans, respectively (Fig. 1b). There is a tendency for in source-prompted facile loss of a sodium sulfite from the disulfated molecular ions, corresponding to a neutral loss of 102 u but not for the monosulfated ones. On the other hand, in positive ion mode, the sulfated glycans preferentially ionize as $[M + (n + 1) Na-nH]^+$, where n = number of sulfates, but in source-prompted multiple losses of sodium sulfite to give ions retaining fewer or none of the sulfate moieties is commonly observed (Fig. 1a).

Taken these into consideration, both positive and negative ion mode MS data as shown in Fig. 1 indicated that the fully disulfated species were indeed the major components, particularly since these were expected to compete less favorably against the monosulfated ones both because of the extra charge and being larger in size. Any desulfation during the sample handling and chemical derivatization would have produced significant amount of neutral glycans that would be preferentially detected in positive ion mode. The absence of such signal is supportive of previously drawn conclusion that our permethylation protocols will not induce appreciable loss of sulfate. Moreover, only a relatively very minor amount of monosulfated biantennary structure with fully extended lacdiNAc termini could be detected, which indicated that a majority of these biantennary structures were in

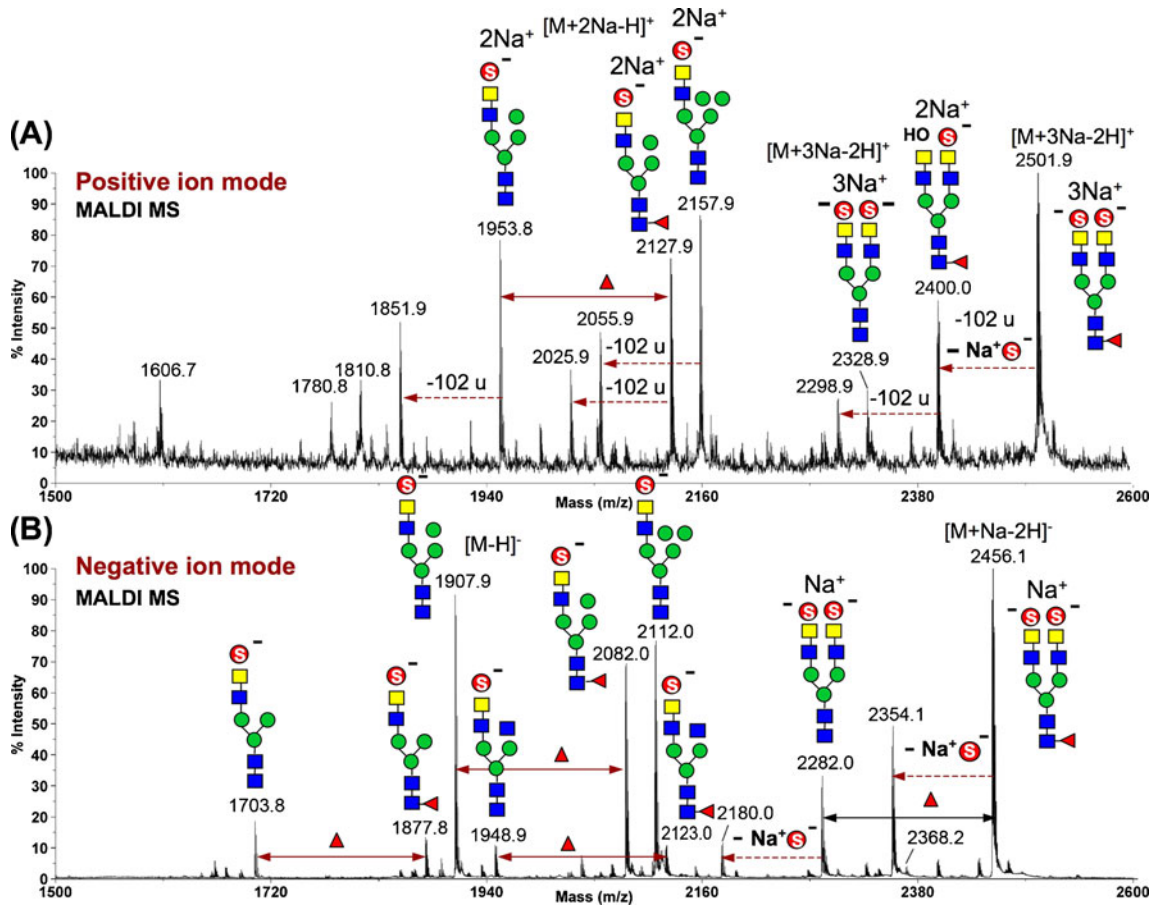

Fig. 1 MALDI-MS profiles of the permethylated N-glycans from bTSH in positive (**a**) and negative (**b**) ion modes. Assignment of the major structures are as annotated using the standard cartoon symbols recommended by the Consortium for Functional Glycomics. In the context of MS analysis, square represents HexNAc, circle for Hex and triangle for Fuc. Most of the structural details other than the glycosyl compositions were assumed from prior knowledge. The overall sequences particularly the terminal epitopes were, however, supported by MS/MS analyses. Loss of sodium sulfite (102 u) was commonly observed in positive ion mode and from the disulfated species in negative ion mode. This would produce species carrying a free OH group for each loss of the sulfate moiety. Thus, for example in negative ion mode, a monosulfated species (*m/z* 2354) derived from a disulfated molecular ion (*m/z* 2456) via in source prompted neutral loss of a sodium sulfite (102 u) can be distinguished from an authentic monosulfated species carried on the same underlying structure (*m/z* 2368), by virtue of the mass difference of 14 u corresponding to a methyl group. In positive ion mode, a neutral loss of sodiated sulfo-HexNAc instead of just the sodium sulfite moiety would generate the ions at *m/z* 1606, 1780, and 1810 from the species at *m/z* 1953, 2127 and 2157, respectively

fact disulfated, whereas the hybrid type N-glycans were mostly monosulfated.

While variations in sample preparation from both the original studies and subsequent commercial sources cannot be discounted, our current data suggest that the degree of sulfation in bTSH is probably higher than previously estimated [14]. It also contrasted with more recent analyses by MS, in which the disulfated species appeared to be underrepresented. In an earlier work analyzing the in-gel released bTSH N-glycans in their native forms in both positive and negative ion modes [33], the loss of sulfation from the di- and monosulfated species, either through sample preparation or in source fragmentation, could not be accurately determined. In other work similarly analyzing the permethylated bTSH N-glycans by MALDI-MS in positive ion mode, very minor amount of disulfated glycans were actually detected by direct analysis [34] and became prominent only after enriching them by ion exchange [35]. We propose that a proper permethylation followed by direct MS screening in negative ion mode such as that employed here represents the best MS-based approach to detect sulfated glycans. We have demonstrated before [8], and herein again using a well-characterized, readily available bTSH source, that sulfates on both lacNAc and lacdiNAc structural units can be rather sensitively and conveniently detected instead of being unduly suppressed or lost during the process.

Characteristic fragment ions defining the presence of 4′-O-sulfo lacdiNAc

Aiming to establish the characteristic fragment ions that would allow unambiguous identification of 4′-O-sulfo lacdiNAc, the major disulfated biantennary glycans from bTSH were subjected to both positive and negative ion mode MS/MS analyses (Fig. 2). As shown previously, MALDI-MS/MS of cation-paired sulfated glycans in positive ion mode will not induce substantial loss of sulfate. Instead, a full range of fragment ions analogous to those afforded by high energy CID MS/MS of non-sulfated glycans would be produced (Fig. 2a). Interestingly, while cleavage at the reducing end of sub-terminal GlcNAc preferentially gave the disodiated E ion at *m/z* 544 instead of the B ion, that at the terminal GalNAc afforded mostly a strong disodiated B ion at *m/z* 370, corresponding to a terminal sulfated HexNAc. However, no fragment ion informative of the exact location of sulfate on the terminal HexNAc could be detected.

In negative ion mode, the presence of sulfate was informed by the highly abundant sulfate anion HSO_4^- at *m/z* 97. More importantly, the 4′-O-sulfo-HexNAc-4HexNAc sequence could be unambiguously established by the prominent fragment ions at *m/z* 167, 324 and 569, corresponding to $^{3,5}A_0$, B_1, and B_2 ions, respectively (Fig. 2b). These were further accompanied by the D ions at *m/z* 310 and 555 and another critical $^{3,5}A_1$ ion at *m/z* 412. The last ion was indicative of the internal 4-linked HexNAc linkage, whereas the ion at *m/z* 167 indicated that the sulfate could only be on the 4 or 6 position of the terminal HexNAc. In the absence of an $^{O,4}A$ ion at *m/z* 139 indicative of 6-O-sulfate, these ions therefore collectively defined the 4′-O-sulfo lacdiNAc glycotope. Other ions of higher *m/z* values could be assigned accordingly as illustrated on Fig. 2b.

It is of interest to note that all fragment ions in negative ion mode would need to retain at least one sulfate group and therefore in the case of monosulfated hybrid type N-glycans, the trios of $^{O,4}A$, $^{3,5}A$ and D ions produced via cleavages at the trimannosyl core would not have been formed and likewise for the Y ions arising through loss of terminal sulfated $HexNAc_1$ or $HexNAc_2$ (data not shown). In addition, it should be added that although these fragment ions were currently produced via high energy CID on a TOF/TOF, a collision energy (1 kV) lower than that required for positive ion mode MS/MS (2-3 kV) was employed, which nevertheless similarly yielded ions such as the A, D and E ions. This was perhaps not surprising since the same phenomenon was observed for low energy CID MS/MS analysis of native glycans in negative ion mode [36–38], which is more prone to give sequence informative ring cleavages and the D ions than in positive ion mode, which favors instead glycosidic cleavages.

Anticipating that some laboratories may only have access to or prefer nanoLC-MS/MS systems relying on low collision energy ion trap or Q/TOF instruments, we have further subjected the same molecular ions to negative ion mode nanoESI-MS^n analysis (Fig. 2c). As expected, the 2 major ions detected by MS^2 were the B ions at *m/z* 991(2-) and 569, corresponding to cleavages at the chitobiose core and the sulfated $HexNAc_2$ moiety, respectively. The ion trap system suffers from the lower mass cut-off problem and thus in this case, ions below *m/z* 400 were not observed. However, the MS^2 ion at *m/z* 569 could be taken through MS^3, which yielded prominent fragment ions at *m/z* 412 and 324, with a minor signal at *m/z* 167 (Fig. 2c, inset). Thus, similar set of diagnostic ions could also be derived by negative ion mode ESI-based MS/MS analysis at low collision energy, which increases their versatility and usefulness. In fact, the ions at *m/z* 324, 412 and 569 were also produced by the same permethylated sulfated lacdiNAc structures under FAB-MS on a sector instrument and the underlying fragmentation mechanisms have been proposed [39]. It is reassuring that despite migrating now to MALDI- and ESI-MS platforms using CID MS/MS instead of direct fragmentation under FAB-MS, the characteristic ions remain the same, which lend support to their use to identify the presence of 4′-*O*-sulfo lacdiNAc. A distinction to be made though is that the B ions at *m/z* 324 and 569 appear to be

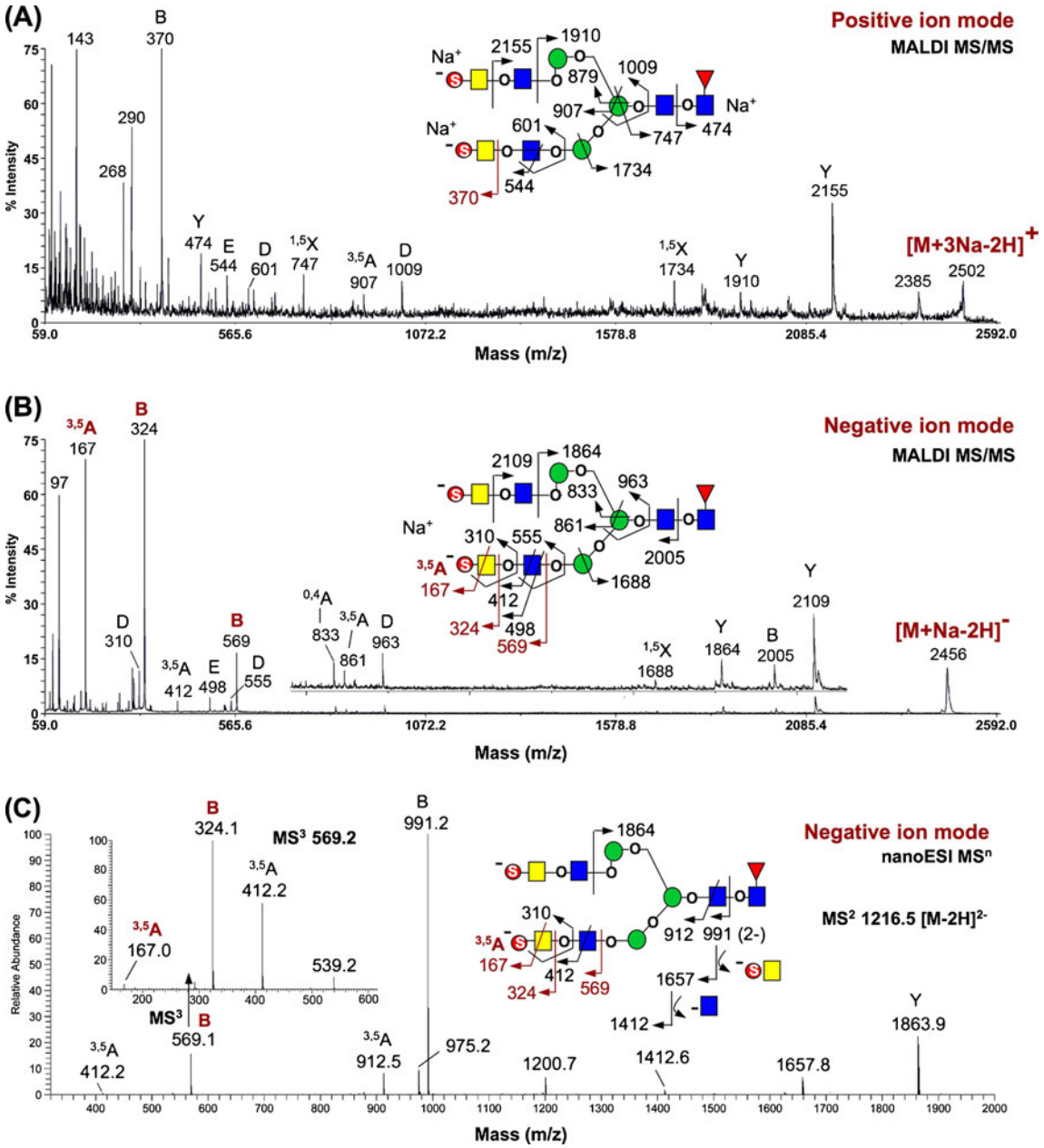

Fig. 2 MALDI-MS/MS profiles of the permethylated disulfated biantennary N-glycan from bTSH in positive (**a**) and negative (**b**) ion modes, and the corresponding nanoESI-MS^n profiles in negative ion mode (**c**). Assignment of the major fragment ions are as illustrated schematically. The fragment ion types were labeled according to the commonly adopted nomenclature as defined previously for the positive mode ions [10]. Analogous ions observed in negative ion mode were similarly named. In positive ion mode (**a**), the non-reducing terminal sulfated fragment ions were disodiated. Further loss of sulfite or sodium sulfite from the B ion at *m/z* 370 yielded the ions at *m/z* 290 and 268, respectively. For nanoESI-MS^n in (**c**), the same structure afforded a doubly charged $[M-2H]^{2-}$ molecular ion. Daughter ions retaining both sulfate groups (*m/z* 912, 991) were likewise observed as doubly charged species but those having lost one sulfate and the corresponding non-reducing terminal ions carrying one sulfate were detected as singly charged species. The inset on (**c**) shows the MS^3 spectrum of the MS^2 ion, *m/z* 569. All fragment ions in (**b**) were likewise singly charged and non-sodiated except the monosodiated, disulfated B ion at *m/z* 2005

dominant in the current setting and hence serve as the most useful diagnostic ions when sample amount is limiting (see later section for applications), whereas the D ions at *m/z* 310 and 555 were more abundant by FAB-MS, along with the E_2 ion at *m/z* 498 and C_1" ions at *m/z* 340, which were barely detected by current CID MS/MS system. On the other hand, *m/z* 167 informative of the location of sulfate was not reported by previous FAB-MS studies.

MALDI-MS mapping of N-glycans derived from RMG-1 cell lysates and identification of terminal sulfated lacdiNAc

In general, the possible occurrence of lacdiNAc is hinted first by extra numbers of HexNAc residues relative to Hex in the assigned glycosyl composition, once those 3 Hex and 2 HexNAc residues contributing to the trimannosyl core are subtracted away. However, it remains possible that the extra HexNAc may occur as single non-reducing terminal HexNAc, either as the bisecting GlcNAc on the trimmanosyl core or due to incomplete galactosylation. In sulfoglycomics in particular, we have found many instances of terminal sulfated GlcNAc as incompletely extended sulfo (sialyl) lacNAc units. Thus an unequivocal identification of a terminal 4′-*O*-sulfo lacdiNAc requires positive detection of i) 2 HexNAc residues in tandem; and ii) sulfate on position 4 of terminal HexNAc. The diagnostic ions described above fulfill these criteria.

Among many other cell lines and immune cells we have screened, the ovarian clear cell carcinoma RMG-1 cells alone stood out to have candidate sulfated lacdiNAc among other sulfated glycotopes. Typical of many other cell lines and tissues, its glycomic profile in positive ion mode afforded only prominent high mannoses and typical complex type N-glycans with several degrees of fucosylation and sialylation on multiple lacNAc units (Fig. 3). No obvious signal that may be attributed to unusual glycotopes could be identified. However, a sodiated molecular ion at *m/z* 2592, with a glycosyl composition corresponding to a biantennary core fucosylated structures terminating with 2 fucosylated lacNAc, was found to be accompanied by signals at 41 u higher. This mass increment corresponded to a Hex substitution by a HexNAc and therefore was indicative of lacdiNAc replacing lacNAc. Thus, the signals at *m/z* 2633 and 2674 would correspond to core fucosylated biantennary structures with one and two fucosylated lacdiNAc antenna, respectively. It remains possible that similar +41n u signals for a majority of other assigned lacNAc-carrying components might have been present. These, however, were buried among the noise and could not be easily verified by such direct MALDI-MS profiling to reveal a full complement of minor glycomic constituents carrying non-substituted, sialylated and/or fucosylated lacdiNAc units.

In contrast, the same unfractionated, permethylated N-glycan sample when screened instead by MALDI-MS analysis in negative ion mode unexpectedly afforded several prominent series of signals including those that could clearly be assigned as carrying one or more sulfated lacdiNAc. Prompted by such observation, a further enrichment of the negatively charged N-glycans by QAE-sephadex column prior to permethylation was undertaken, which led to a rather similar negative ion mode spectrum but with much improved signal-to-noise ratio, particularly for the larger, minor components otherwise not observed (Fig. 4).

The first category of the detected negative ion signals corresponded to high mannose structures carrying 1–2 phosphates, which we have similarly observed with several other cell lines particularly those without significant level of sulfated glycans. As reported previously, despite similar nominal mass, a phosphate substituent can be distinguished from sulfate by virtue of being susceptible to add on a methyl group upon permethylation. We have consistently observed that $Hex_{6\text{-}8}HexNAc_2$ were the most abundant species carrying a single phosphate while $Hex_7HexNAc_2$ was the most abundant one carrying 2 phosphates. In addition, a prominent $Hex_6HexNAc_3$ was detected. Such compositions were fully consistent with the detected species being high mannose type N-glycans carrying an extra PO_4- or GlcNAc-PO_4- group on the 6-position of Man, a commonly found modification mediating the uptake and trafficking of lysosomal enzymes by the Man-6-phosphate receptor [40, 41]. The location of a phosphate on the high mannose structures could be further confirmed by MS/MS analyses of select peaks, as exemplified by the data acquired on the diphosphorylated $Hex_7HexNAc_2$ structure (Fig. 5a) in which the ^{3,5}A ion at *m/z* 181, E ion at *m/z* 267 and B ion at *m/z* 297 collectively defined a terminal Hex phosphorylated at either 4 or 6 position.

The second category of signals could be assigned to complex type N-glycans carrying only the normal sulfated sialyl lacNAc epitopes. It was clear that many of these signals were accompanied by signals at 41 u increments, corresponding to aforementioned substitution of a Hex by HexNAc and thus indicative of lacdiNAc. For example, the $[M\text{-}H]^-$ signal at *m/z* 2501 could be assigned as monosulfated, core fucosylated biantennary glycans with an additional Fuc, a lacNAc and a lacdiNAc, whereas the signal at 41 u higher at *m/z* 2542 would correspond to the same core structure but with 2 lacdiNAc instead. Further MALDI-MS/MS analysis (Fig. 5b) afforded strong ions at *m/z* 167, 324 and weaker ions at *m/z* 555, 569, all of which were diagnostic of a terminal 4′-*O*-sulfo lacdiNAc. Likewise the signal at *m/z* 2647 was assigned as monosulfated, core fucosylated biantennary glycans with 2 lacNAc and a sialic acid, whereas the signal at 41 u higher at *m/z* 2688 corresponded to one with a lacNAc, a lacdiNAc and a sialic acid. Interestingly, MALDI-MS/MS analysis (Fig. 5c) afforded the characteristic ions at *m/z* 167, 324 and 569, consistent with the presence of 4′-*O*-sulfo lacdiNAc but not a sulfated lacNAc sequence. Thus the lacdiNAc unit was preferentially sulfated whereas the lacNAc unit was sialylated. This and all other peaks detected indicated that the sulfated lacdiNAc sequence can co-exist with sulfated and/or sialylated lacNAc sequence. Trimming away the sialic acids by sialidase collapsed most of the heterogeneity and the recovered N-glycans

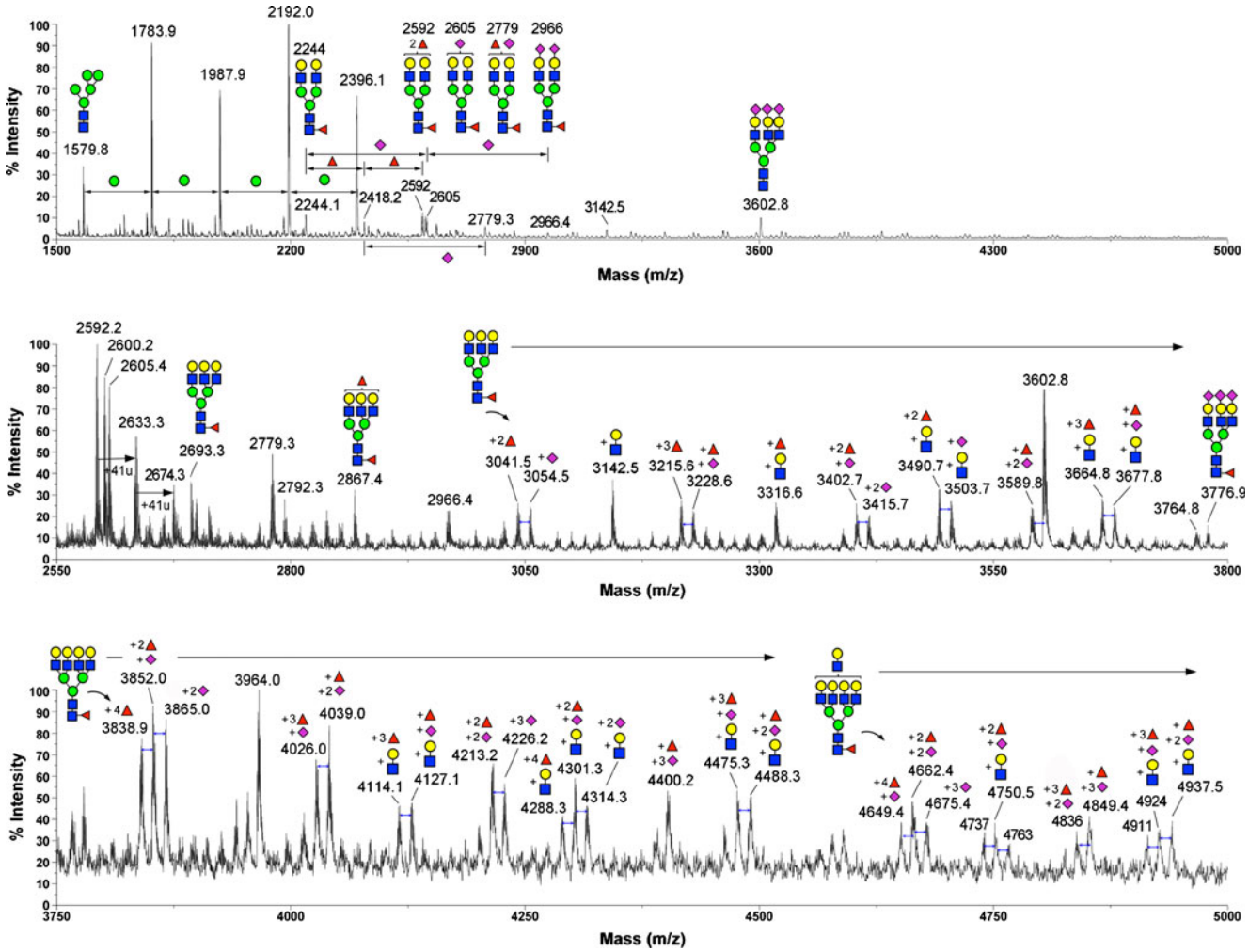

Fig. 3 MALDI-MS profile of the permethylated N-glycans from RMG-1 cells in positive ion mode. The top panel shows a full spectrum, which is clearly dominated by high mannose type structures and likely to be contaminated by the typical non-core fucosylated, disialylated biantennary (*m/z* 2792) and tri- (*m/z* 3602) and tetrasialylated (*m/z* 3964) triantennary structures derived from bovine fetuin in the culture medium. All other detected major $[M+Na]^+$ molecular ion signals could be assigned as core fucosylated multiantennary complex type structures, as annotated in 2 separate segments of expanded mass range (middle and bottom panels) based solely on inferred glycosyl composition without further verification. A mass difference of 13 u, corresponding to substituting 2 Fuc for a single NeuAc, is apparent throughout the spectra, as indicated by double-headed arrows linking the pairs of signals. Any signal at 41 u higher than those assigned, which would correspond to lacdiNAc substituting lacNAc, cannot be clearly identified from the noise level except for the 2 signals at *m/z* 2633 and 2674

were clearly left with those carrying 2–4 lacNAc, with 0–2 degrees of lacdiNAc (data not shown). Such structures may have been identified on other secreted endogenous human glycoproteins but, to our knowledge, were first described here as glycomic constituents of a cell.

It remains to be determined if the sulfated lacdiNAc-carrying glycoproteins were derived from intracellular pool of secreted glycoproteins residing in transient in Golgi lumen, lysosome or other vesicles, rather than authentic membrane glycoproteins. In the same vein, previous studies on high mannose and hybrid type structures released by endo-H from total glycoproteins of cell lysates have led to identification of those phosphorylated high mannose structures, which were assumed to be derived from the lysosomal enzymes [40, 41]. Current glycomic mapping approaches tend not to distinguish these alternatives but regardless, we have identified RMG-1 cell, which was not previously reported to secrete any glycoprotein carrying sulfated lacdiNAc, as capable of synthesizing this sulfated epitope.

Concluding summary

Rapid glycomic identification of sulfated glycotopes remains an important analytical challenge to be met. Whilst much focus has naturally been devoted to various combinations of

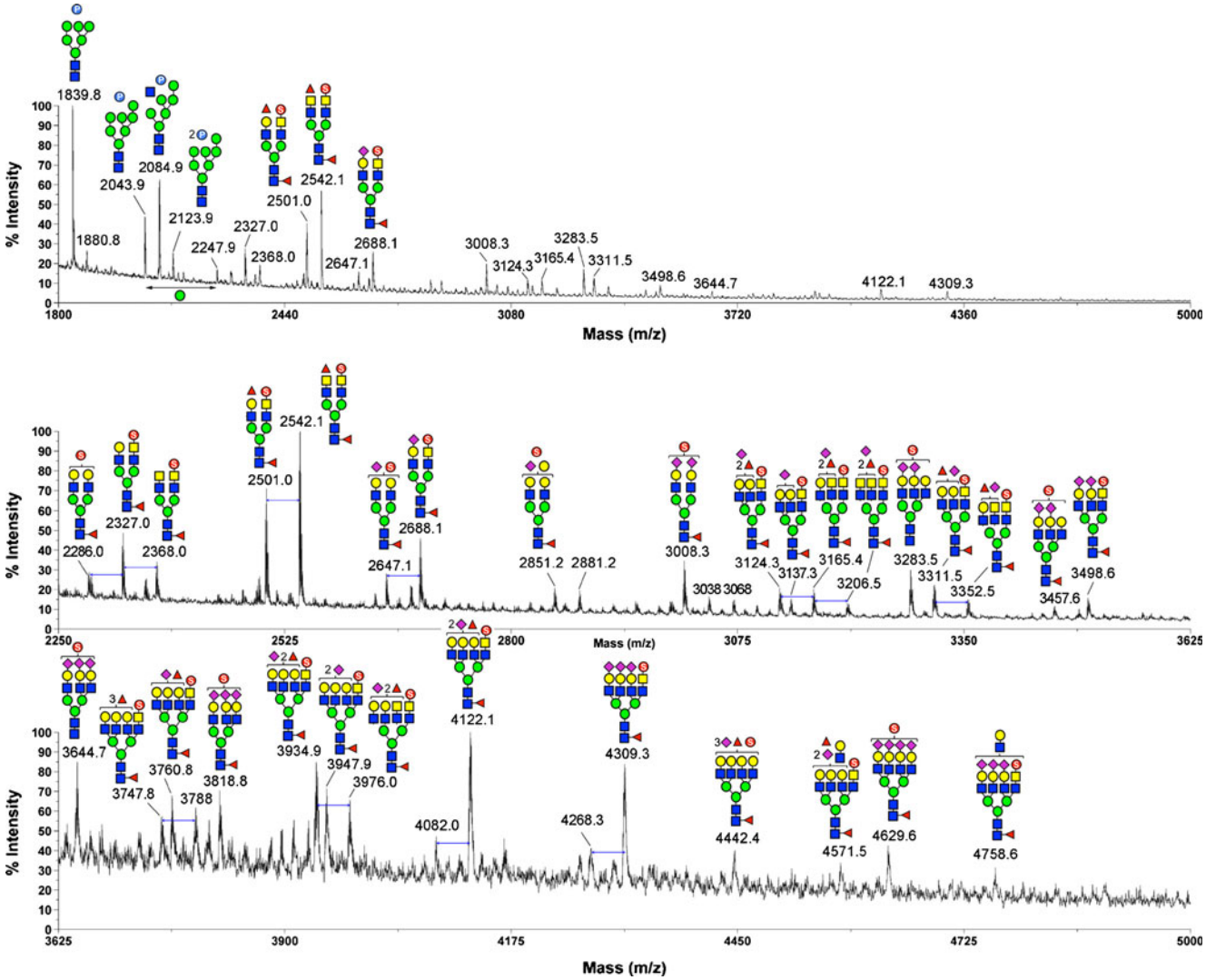

Fig. 4 MALDI-MS profile of the permethylated N-glycans from RMG-1 cells in negative ion mode. The top panel shows a full spectrum. The major negatively charged components are the phosphorylated $Man_{6\text{-}7}GlcNAc_2$ structures and the biantennary fucosylated or sialylated complex type structures with one sulfated lacdiNAc antenna. The former includes an $[M\text{-}H]^-$ molecular ion for a di-phosphorylated $Man_7GlcNAc_2$ structure, which gave a doubly charged $[M\text{-}2H]^{2-}$ by nanoESI-MS analysis and MS^2 ions consistent with the assignment (Fig. 5a). All other major $[M\text{-}H]^-$ molecular ion signals detected could be assigned as monosulfated core fucosylated multiantennary complex type structures, as annotated in 2 separate segments of expanded mass range (middle and bottom panels), based solely on inferred glycosyl composition. Many +41 u signals could be observed and indicated here with double-headed arrows, which could be translated into structures carrying 1-3 lacdiNAc units alongside lacNAc. No attempt was made to verify each structure or to distinguish GalNAc from GlcNAc. Select MALDI-MS/MS were performed (Fig. 5) instead to simply identify the probable presence of the sulfated lacdiNAc glycotopes under investigation based on the established diagnostic ions

sulfo sialyl lacNAc or Lewis X in the context of mediating lymphocyte homing [42, 43], other epitopes such as the sulfated lacdiNAc investigated here are equally important with many functional implications. Despite it being well characterized on pituitary glycohormones and several other secreted glycoproteins, a possible wider occurrence of sulfated lacdiNAc on other cells and tissues is unclear. We now showed that the ovarian carcinoma cells RMG-1 display an abundance of this epitope alongside sulfated and/or sialylated lacNAc on multi-antennary complex type N-glycans. In contrast, non-sulfated lacdiNAc including fucosylated lacdiNAc appears to be expressed only at much lower level relative to other terminal sequences. It suggests that in cells expressing the requisite sulfotransferase, terminal GalNAc 4-*O*-sulfation of lacdiNAc occurs rather efficiently, in preference over terminal sialylation and additional fucosylation.

Occurrence of lacdiNAc has also been recently reported for another ovarian carcinoma cell line SKOV3 but the possibility of a higher abundance of sulfated lacdiNAc or indeed any sulfated glycan has not been considered [21].

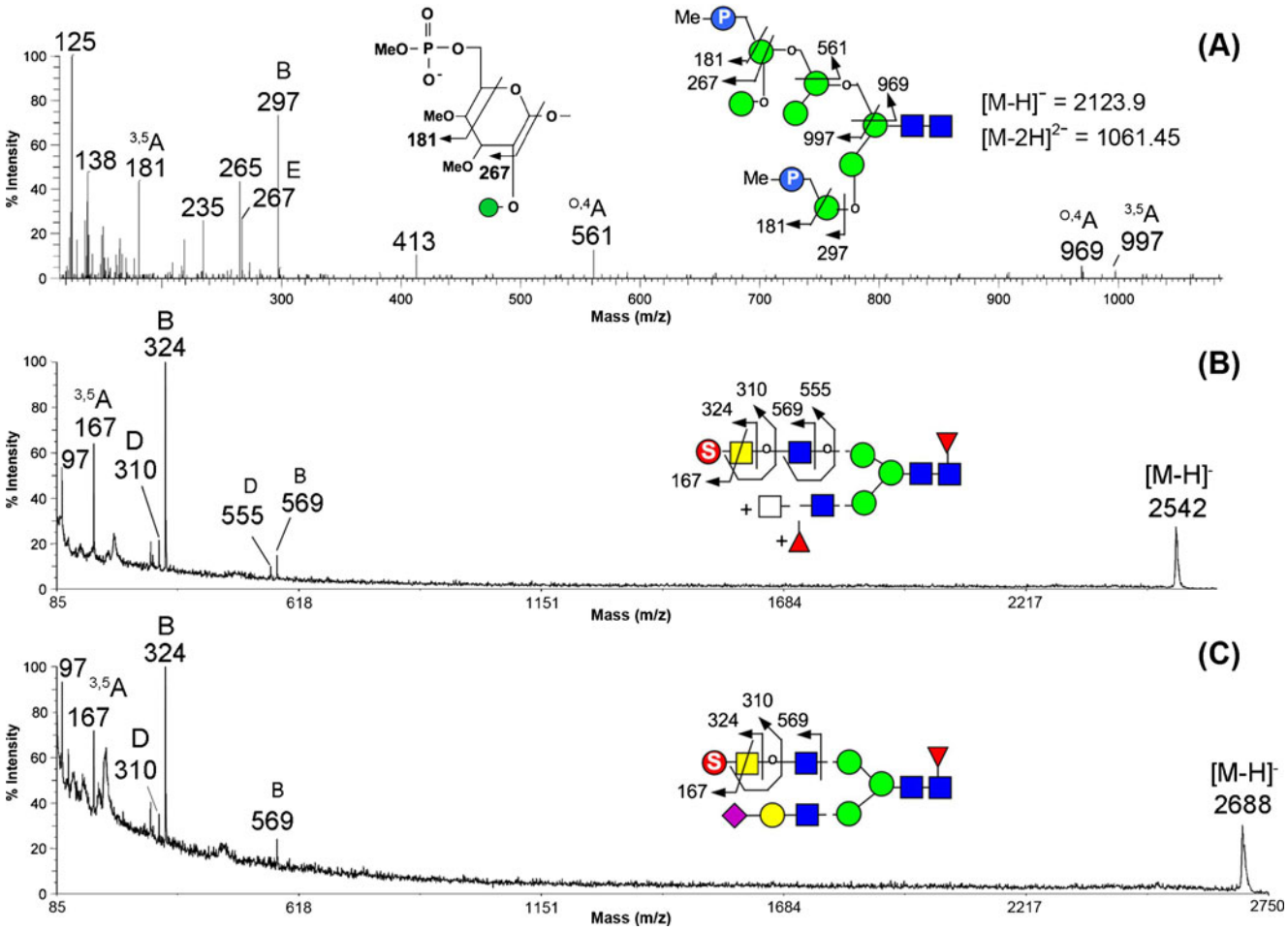

Fig. 5 Select MS/MS profiles of negatively charged permethylated N-glycans from RMG-1 demonstrating the presence of a Man-6-phosphate on a high mannose structure (**a**) and sulfated lacdiNAc on a non-sialylated (**b**) and sialylated (**c**) biantennary complex type structures. The nanoESI-MS/MS spectrum in (**a**) was acquired for the doubly charged parent ion under HCD mode to avoid low mass cutoff, which also gave a better sensitivity and more sequence informative ring cleavage ions than MALDI-MS/MS (not shown). Both the B and E ions at *m/z* 297 and 267 were accompanied by loss of MeOH moiety (- 32 u) to give ions at *m/z* 265 and 235, respectively. Despite lack of other cleavage ions, MALDI-MS/MS did give a very prominent ion at *m/z* 324 accompanied by other critical ions at *m/z* 167 and 569 to allow rapid identification of terminal sulfated lacdiNAc epitope during initial screening. No B ion could be detected to suggest alternative location of sulfate on the other sialylated or fucosylated antenna. Such non-sulfated antennae would not be expected to give any fragment ion in negative ion mode and therefore their exact sequence could not be confirmed. The fucosylated $HexNAc_2$ sequence in (**b**) is most likely a fucosylated lacdiNAc as tentatively annotated in Fig. 4 but MS/MS alone cannot distinguish GalNAc from GlcNAc, nor the exact location of Fuc in this case

In contrast, RMG-1 cells have been used to raise a humanized monoclonal antibody recently shown to be active against sulfated lacNAc-based glycotopes [30], consistent with our current sulfoglycomic mapping showing the presence of a full range of sulfated glycotopes in addition to sulfated lacdiNAc. RMG-1 and other ovarian cancer cell lines would serve as good model cell lines to further investigate the activity of the implicated GalNAc-4-sulfotransferase, its likely ectopic expression, and the functional relevance of sulfated lacdiNAcs other than mediating clearance of glycohormones. On the other hand, our finding also serves as a cautionary tale against using RMG-1 as a model cell line for other glycobiology investigations due to the prominent presence of this epitope which may mislead data interpretations.

Technique wise, we have established the critical ions that, in negative ion mode, can collectively identify the presence of sulfated lacdiNAc at reasonably high sensitivity by MALDI-MS/MS. We further showed that the same ions could also be produced by nanoESI-MS/MS but one needs to be aware of the low mass cutoff if using an ion trap system instead of a Q/TOF system or employing the HCD mode on the orbitrap series. However, the ion at *m/z* 569 can be further taken through MS^3 to give ions at *m/z* 324 and 167. A caveat though is that detection by such diagnostic ions actually does not critically distinguish terminal sulfated

GalNAc from GlcNAc, which would require further confirmation by other chemical and chromatography methods should the sample amount be sufficient. Incidentally, we have also identified the phosphorylated high mannose type structures, which were often found to exist along with the sulfated glycans when screening the permethylated glycans in negative ion mode. The terminal phosphorylated Man likewise afforded diagnostic ions distinct from those of sulfated lacdiNAc, or other sulfated sialylated lacNAc epitopes. We are now incorporating these ions in LC-MS/MS approach in which data dependent acquisition can be followed by MS^2 product ion filtering to selectively identify parent ions with such epitopes. Furthermore, product ion dependent MS^3 can be selectively triggered to further confirm location of sulfate. Finally, we provided an updated glycomic analysis of the bTSH, which shall continue to serve as gold standard for others to further optimize the technical aspects of an unbiased sulfoglycomic mapping.

Acknowledgements This work was supported by Academia Sinica and Taiwan National Science Council (NSC) grant 99-2311-B-001-021-MY3 (to KKH), and an NIH grant CA 33895 (to MNF). The MS data were acquired at the previous NRPGM Core Facilities for Proteomics and Glycomcis (NSC 99-3112-B-001-025; 98-3112-B-001-023), and current Core Facilities for Protein Structural Analysis at Academia Sinica, supported under the Taiwan National Core Facility Program for Biotechnology, NSC 100-2325-B-001-029.

References

1. Hart, G.W., Copeland, R.J.: Glycomics hits the big time. Cell **143**, 672–676 (2010)
2. Zaia, J.: Mass spectrometry and glycomics. OMICS **14**, 401–418 (2010)
3. Jang-Lee, J., North, S.J., Sutton-Smith, M., Goldberg, D., Panico, M., Morris, H., Haslam, S., Dell, A.: Glycomic profiling of cells and tissues by mass spectrometry: fingerprinting and sequencing methodologies. Methods Enzymol **415**, 59–86 (2006)
4. North, S.J., Hitchen, P.G., Haslam, S.M., Dell, A.: Mass spectrometry in the analysis of N-linked and O-linked glycans. Curr Opin Struct Biol **19**, 498–506 (2009)
5. Telford, J.E., Doherty, M.A., Tharmalingam, T., Rudd, P.M.: Discovering new clinical markers in the field of glycomics. Biochem Soc Trans **39**, 327–330 (2011)
6. Kolarich, D., Lepenies, B., Seeberger, P.H.: Glycomics, glycoproteomics and the immune system. Curr Opin Chem Biol (2012)
7. Khoo, K.H., Yu, S.Y.: Mass spectrometric analysis of sulfated N- and O-glycans. Methods Enzymol **478**, 3–26 (2010)
8. Yu, S.Y., Wu, S.W., Hsiao, H.H., Khoo, K.H.: Enabling techniques and strategic workflow for sulfoglycomics based on mass spectrometry mapping and sequencing of permethylated sulfated glycans. Glycobiology **19**, 1136–1149 (2009)
9. Dell, A.: F.A.B.-mass spectrometry of carbohydrates. Adv Carbohydr Chem Biochem **45**, 19–72 (1987)
10. Yu, S.Y., Wu, S.W., Khoo, K.H.: Distinctive characteristics of MALDI-Q/TOF and TOF/TOF tandem mass spectrometry for sequencing of permethylated complex type N-glycans. Glycoconj J **23**, 355–369 (2006)
11. Wada, Y., Azadi, P., Costello, C.E., Dell, A., Dwek, R.A., Geyer, H., Geyer, R., Kakehi, K., Karlsson, N.G., Kato, K., Kawasaki, N., Khoo, K.H., Kim, S., Kondo, A., Lattova, E., Mechref, Y., Miyoshi, E., Nakamura, K., Narimatsu, H., Novotny, M.V., Packer, N.H., Perreault, H., Peter-Katalinic, J., Pohlentz, G., Reinhold, V.N., Rudd, P.M., Suzuki, A., Taniguchi, N.: Comparison of the methods for profiling glycoprotein glycans–HUPO Human Disease Glycomics/Proteome Initiative multi-institutional study. Glycobiology **17**, 411–422 (2007)
12. Mitoma, J., Bao, X., Petryanik, B., Schaerli, P., Gauguet, J.M., Yu, S.Y., Kawashima, H., Saito, H., Ohtsubo, K., Marth, J.D., Khoo, K.H., von Andrian, U.H., Lowe, J.B., Fukuda, M.: Critical functions of N-glycans in L-selectin-mediated lymphocyte homing and recruitment. Nat Immunol **8**, 409–418 (2007)
13. Kobayashi, M., Mitoma, J., Hoshino, H., Yu, S.Y., Shimojo, Y., Suzawa, K., Khoo, K.H., Fukuda, M., Nakayama, J.: Prominent expression of sialyl Lewis X-capped core 2-branched O-glycans on high endothelial venule-like vessels in gastric MALT lymphoma. J Pathol **224**, 67–77 (2011)
14. Baenziger, J.U., Green, E.D.: Pituitary glycoprotein hormone oligosaccharides: structure, synthesis and function of the asparagine-linked oligosaccharides on lutropin, follitropin and thyrotropin. Biochim Biophys Acta **947**, 287–306 (1988)
15. Baenziger, J.U.: Glycoprotein hormone GalNAc-4-sulphotransferase. Biochem Soc Trans **31**, 326–330 (2003)
16. Van den Eijnden, D.H., Neeleman, A.P., Van der Knaap, W.P., Bakker, H., Agterberg, M., Van Die, I.: Novel glycosylation routes for glycoproteins: the lacdiNAc pathway. Biochem Soc Trans **23**, 175–179 (1995)
17. Do, K.Y., Do, S.I., Cummings, R.D.: Differential expression of LacdiNAc sequences (GalNAc beta 1-4GlcNAc-R) in glycoproteins synthesized by Chinese hamster ovary and human 293 cells. Glycobiology **7**, 183–194 (1997)
18. Ohkura, T., Seko, A., Hara-Kuge, S., Yamashita, K.: Occurrence of secretory glycoprotein-specific GalNAc beta 1–>4GlcNAc sequence in N-glycans in MDCK cells. J Biochem **132**, 891–901 (2002)
19. Sato, T., Gotoh, M., Kiyohara, K., Kameyama, A., Kubota, T., Kikuchi, N., Ishizuka, Y., Iwasaki, H., Togayachi, A., Kudo, T., Ohkura, T., Nakanishi, H., Narimatsu, H.: Molecular cloning and characterization of a novel human beta 1,4-N-acetylgalactosaminyltransferase, beta 4GalNAc-T3, responsible for the synthesis of N, N′-diacetyllactosediamine, galNAc beta 1–4GlcNAc. J Biol Chem **278**, 47534–47544 (2003)
20. Lee, C.L., Pang, P.C., Yeung, W.S., Tissot, B., Panico, M., Lao, T.T., Chu, I.K., Lee, K.F., Chung, M.K., Lam, K.K., Koistinen, R., Koistinen, H., Seppala, M., Morris, H.R., Dell, A., Chiu, P.C.: Effects of differential glycosylation of glycodelins on lymphocyte survival. J Biol Chem **284**, 15084–15096 (2009)
21. Machado, E., Kandzia, S., Carilho, R., Altevogt, P., Conradt, H.S., Costa, J.: N-Glycosylation of total cellular glycoproteins from the human ovarian carcinoma SKOV3 cell line and of recombinantly expressed human erythropoietin. Glycobiology **21**, 376–386 (2011)
22. Sasaki, N., Shinomi, M., Hirano, K., Ui-Tei, K., Nishihara, S.: LacdiNAc (GalNAcbeta1-4GlcNAc) contributes to self-renewal of mouse embryonic stem cells by regulating leukemia inhibitory factor/STAT3 signaling. Stem Cells **29**, 641–650 (2011)
23. Woodworth, A., Fiete, D., Baenziger, J.U.: Spatial and temporal regulation of tenascin-R glycosylation in the cerebellum. J Biol Chem **277**, 50941–50947 (2002)
24. Hooper, L.V., Beranek, M.C., Manzella, S.M., Baenziger, J.U.: Differential expression of GalNAc-4-sulfotransferase and GalNAc-transferase results in distinct glycoforms of carbonic anhydrase VI in parotid and submaxillary glands. J Biol Chem **270**, 5985–5993 (1995)

25. Bergwerff, A.A., Van Oostrum, J., Kamerling, J.P., Vliegenthart, J.F.: The major N-linked carbohydrate chains from human urokinase. The occurrence of 4-O-sulfated, (α 2-6)-sialylated or (α 1-3)-fucosylated N-acetylgalactosamine(beta 1-4)-N-acetylglucosamine elements. Eur J Biochem **228**, 1009–1019 (1995)
26. van Rooijen, J.J., Kamerling, J.P., Vliegenthart, J.F.: Sulfated di-, tri- and tetraantennary N-glycans in human Tamm-Horsfall glycoprotein. Eur J Biochem **256**, 471–487 (1998)
27. Smith, P.L., Skelton, T.P., Fiete, D., Dharmesh, S.M., Beranek, M.C., MacPhail, L., Broze Jr., G.J., Baenziger, J.U.: The asparagine-linked oligosaccharides on tissue factor pathway inhibitor terminate with SO4-4GalNAc beta 1, 4GlcNAc beta 1,2 Mana alpha. J Biol Chem **267**, 19140–19146 (1992)
28. Boregowda, R.K., Mi, Y., Bu, H., Baenziger, J.U.: Differential expression and enzymatic properties of GalNAc-4-sulfotransferase-1 and GalNAc-4-sulfotransferase-2. Glycobiology **15**, 1349–1358 (2005)
29. Green, E.D., Baenziger, J.U.: Asparagine-linked oligosaccharides on lutropin, follitropin, and thyrotropin. I. Structural elucidation of the sulfated and sialylated oligosaccharides on bovine, ovine, and human pituitary glycoprotein hormones. J Biol Chem **263**, 25–35 (1988)
30. Shibata, T.K., Matsumura, F., Wang, P., Yu, S., Chou, C.C., Khoo, K.H., Kitayama, K., Akama, T.O., Sugihara, K., Kanayama, N., Kojima-Aikawa, K., Seeberger, P.H., Fukuda, M., Suzuki, A., Aoki, D., Fukuda, M.N.: Identification of mono- and disulfated N-Acetyl-lactosaminyl oligosaccharide structures as epitopes specifically recognized by humanized monoclonal antibody HMOCC-1 raised against ovarian cancer. J Biol Chem **287**, 6592–6602 (2012)
31. Hiraoka, N., Petryniak, B., Nakayama, J., Tsuboi, S., Suzuki, M., Yeh, J.C., Izawa, D., Tanaka, T., Miyasaka, M., Lowe, J.B., Fukuda, M.: A novel, high endothelial venule-specific sulfotransferase expresses 6-sulfo sialyl Lewis(x), an L-selectin ligand displayed by CD34. Immunity **11**, 79–89 (1999)
32. Green, E.D., Baenziger, J.U.: Asparagine-linked oligosaccharides on lutropin, follitropin, and thyrotropin. II. Distributions of sulfated and sialylated oligosaccharides on bovine, ovine, and human pituitary glycoprotein hormones. J Biol Chem **263**, 36–44 (1988)
33. Wheeler, S.F., Harvey, D.J.: Extension of the in-gel release method for structural analysis of neutral and sialylated N-linked glycans to the analysis of sulfated glycans: application to the glycans from bovine thyroid-stimulating hormone. Anal Biochem **296**, 92–100 (2001)
34. Lei, M., Mechref, Y., Novotny, M.V.: Structural analysis of sulfated glycans by sequential double-permethylation using methyl iodide and deuteromethyl iodide. J Am Soc Mass Spectrom **20**, 1660–1671 (2009)
35. Lei, M., Novotny, M.V., Mechref, Y.: Sequential enrichment of sulfated glycans by strong anion-exchange chromatography prior to mass spectrometric measurements. J Am Soc Mass Spectrom **21**, 348–357 (2010)
36. Thomsson, K.A., Karlsson, H., Hansson, G.C.: Sequencing of sulfated oligosaccharides from mucins by liquid chromatography and electrospray ionization tandem mass spectrometry. Anal Chem **72**, 4543–4549 (2000)
37. Robbe, C., Capon, C., Coddeville, B., Michalski, J.C.: Diagnostic ions for the rapid analysis by nano-electrospray ionization quadrupole time-of-flight mass spectrometry of O-glycans from human mucins. Rapid Commun Mass Spectrom **18**, 412–420 (2004)
38. Harvey, D.J.: Structural determination of N-linked glycans by matrix-assisted laser desorption/ionization and electrospray ionization mass spectrometry. Proteomics **5**, 1774–1786 (2005)
39. Dell, A., Morris, H.R., Greer, F., Redfern, J.M., Rogers, M.E., Weisshaar, G., Hiyama, J., Renwick, A.G.: Fast-atom-bombardment mass spectrometry of sulphated oligosaccharides from ovine lutropin. Carbohydr Res **209**, 33–50 (1991)
40. Varki, A., Kornfeld, S.: Structural studies of phosphorylated high mannose-type oligosaccharides. J Biol Chem **255**, 10847–10858 (1980)
41. Varki, A., Kornfeld, S.: The spectrum of anionic oligosaccharides released by endo-beta-N-acetylglucosaminidase H from glycoproteins. Structural studies and interactions with the phosphomannosyl receptor. J Biol Chem **258**, 2808–2818 (1983)
42. Kawashima, H.: Roles of sulfated glycans in lymphocyte homing. Biol Pharm Bull **29**, 2343–2349 (2006)
43. Rosen, S.D.: Ligands for L-selectin: homing, inflammation, and beyond. Annu Rev Immunol **22**, 129–156 (2004)